SEA ICE MOTION FROM SPACE: AN ALTERNATIVE METHOD AND ITS VALIDATION IN THE ARCTIC

Thomas Lavergne, Steinar Eastwood, Johannes Roërs, Harald Schyberg, and Lars-Anders Breivik

Norwegian Meteorological Institute, Norway

ABSTRACT

We present a sea ice motion tracking algorithm tailored for observing the drift of Arctic sea ice using, among others, the ASCAT instrument on board the European polar orbiting platform Metop. Based on the well known Maximum Cross-Correlation (MCC), the method allows for observing sea ice displacements over shorter time spans (2 days) from low resolution (10–15 km) active and passive microwave imaging sensors. Indeed, the Continuous MCC (CMCC) relies on a continuous optimization step for computing the components of the motion vector, that removes the quantization noise. The resulting 48-hour motion fields look spatially consistent and are not plagued by the usual MCC artifacts (poor angular resolution, large regions with zero-length vectors, etc...).

Results from a validation exercise against GPS trajectories of in situ drifters over several Arctic winters are also presented. They document an unbiased agreement between the products obtained from the satellite sensors (ASCAT, SSM/I and AMSR-E) and the in situ dataset, with standard deviations ranging from 2.5 to 4.5 km, thus achieving sub-pixel accuracy.

The operational EUMETSAT OSI SAF sea ice drift product is based on the algorithms described in this paper.

Key words: sea ice motion; CMCC; EUMETSAT OSI SAF.

1. INTRODUCTION

Sea ice motion information from low resolution satellite sensors (e.g. SSM/I, AMSR-E and ASCAT) can greatly benefit operational coupled ocean and ice models via Data Assimilation (DA) techniques. These models and assimilation systems have recently been developped for operational forecasting of the ocean and ice conditions at daily to seasonal scales, as well as to allow re-analysis experiments. Examples of such systems are TOPAZ (Bertino & Lisæter 2008), the Met Office FOAM (Stark et al. 2008) or the NAOSIMDAS system (Kauker et al. 2009), among others.

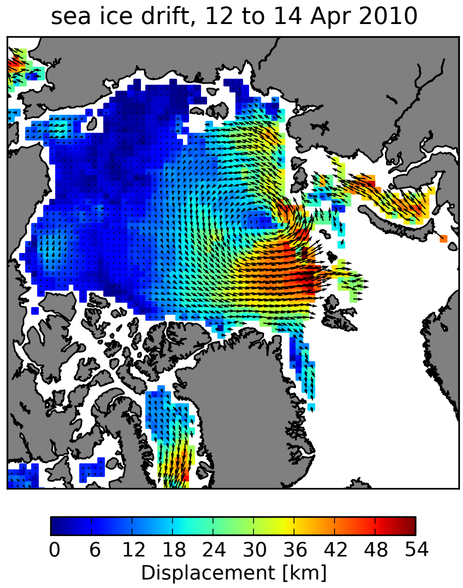

Figure 1. CMCC-based sea ice drift vectors from 12 to 14 April 2010 processed by the EUMETSAT OSI SAF.

For efficient initialization of their forecast cycle, these large scale models need accurate, spatially and temporally covering sea ice motion information, furthermore available in near-real-time. For the time being, such an information cannot solely be provided by the few drifting buoys deployed on the ice, e.g. those from the International Arctic Buoy Programme (IABP) nor from the high-resolution ice motion derived from SAR instruments, which might not be spatially and temporally covering (e.g. `www.seaice.dk`).

On the other hand, the low resolution (10–15 km) of the images recorded by the SSM/I, AMSR-E or ASCAT instruments limit the accuracy one can expect for sea ice motion datasets retrieved by cross-correlation of such image pairs. This is particularly true if the well known Maximum Cross-Correlation (MCC) method is used, since the typical daily displacement of Arctic sea ice is of the same order of magnitude than few image pixels. This implies a dominating quantization noise, characterized by large areas of zero-length vectors or abrupt changes in the direction of the motion vectors.

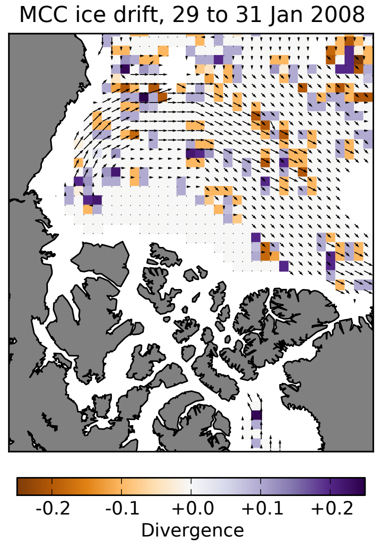

Figure 2. Example MCC-based ice displacements from AMSR-E (37 GHz H&V channels) over the Beaufort Sea and Canadian Basin from 29 to 31 January 2008. The shades of red (blue) colour indicate areas of local convergence (divergence).

In this paper, we present an alternative motion tracking method that removes this quantization noise and allows processing spatially consistent 48-hour ice motion fields in the Arctic from the same satellite images. This algorithm was implemented in the operational processing chain of the EUMETSAT Ocean and Sea Ice Satellite Application Facility (OSI SAF, `www.osi-saf.org`) that delivers daily ice motion products, whose specifications are introduced here. Finally, results from a validation exercise against GPS drifters are briefly summarized both following a Eulerian and Lagrangian approach.

2. SEA ICE MOTION TRACKING

Similarly to other motion tracking applications in geoscience (sea surface currents, winds, etc...), sea ice motion vectors are computed by cross-correlation of pairs of satellite images. By far the most widely used, the Maximum Cross Correlation (MCC) technique is a block-based motion estimation method which repeatedly evaluates the cross-correlation between two sub-images, one taken from the "begin" image (reference block) and the other from the "end" image (candidate block). Each motion vector is optimized separately from its neighbors, and is the pair of offset pixel numbers (δ_x,δ_y) = (i,j) where the maximum cross-correlation occurs. The reader is referred to the description of Notarstefano et al. (2007), among others. The discrete nature of the MCC algorithm necessarily results in a quantization noise, which dominates more or less the signal, depending on the relative magnitude of the typical displacement length to the resolution of the images used.

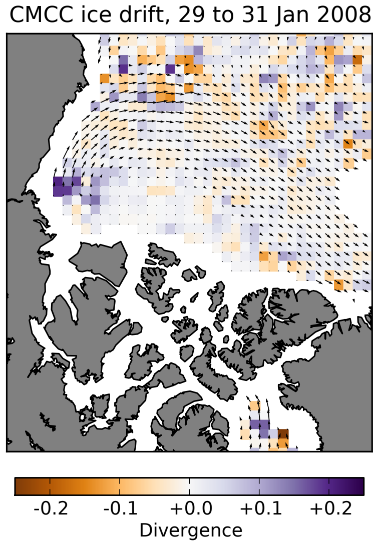

Figure 3. Same as figure 2 but processing the same AMSR-E images with the Continuous Maximum Cross-Correlation (CMCC) instead of with the MCC.

Based on the MCC, we designed a continuous method for optimizing the cross-correlation function. The novel method is accordingly named the Continuous MCC (CMCC). The crux of the method is in computing the cross-correlation function at any (δ_x,δ_y) pair[1] in the 2D space of x (y) components of the motion vector. In our implementation, this is tackled by a bi-linear interpolation of "virtual" image pixels from the original "begin" image. The optimization of the cross-correlation function $\rho(\delta_x, \delta_y)$ is achieved by a simplex algorithm (Nelder & Mead 1968).

The prime effect of adopting a continuous optimization of $\rho(\delta_x, \delta_y)$ is the removal of the quantization noise. Figures 2 and 3 illustrate this effect. On figure 2 (resp. figure 3), sea ice motion derived using the MCC (resp. CMCC) is displayed. Both correspond to the displacement of sea ice from 29 to 31 January 2008 over the Beaufort Sea and Canadian Basin. Both motion fields are computed from the same 12.5 km resolution images recorded by the 37 GHz channels of the AMSR-E instrument on board the NASA Aqua platform. With the MCC (figure 2), the motion field is dominated by a strong quantization noise, with large areas exhibiting zero-length or exactly parallel ice motion. This artefact is not visible on the CMCC-based motion field (figure 3), that seems spatially smoother.

Still on figures 2 and 3, shades of red (blue) colour indicate areas of local convergence (divergence). The quantization noise induced by the MCC translates in sharp changes in the direction of the motion vectors and, thus, to spurious divergence or convergence events. Inside the areas where the MCC motion vectors are parallel, the divergence is exactly zero which is not a realistic value.

[1] As opposed to the discrete (i,j) resulting from the MCC.

Further algorithm developments allow for optimally blending the information content of several imaging channels (e.g. SSM/I 85 GHz H.-pol. and V.-pol.) into a unique vector and to detect and correct ”rogue” motion vectors that are due to noise in the images.

Interested users are referred to Lavergne et al. (2010) for more details on the CMCC method.

3. OPERATIONAL IMPLEMENTATION AT THE EUMETSAT OSI SAF

The algorithms introduced above were implemented in the operational chain of the EUMETSAT Ocean and Sea Ice Satellite Application Facility (OSI SAF, `www.osi-saf.org`).

The OSI SAF is a consortium led by Météo-France, with a High Latitude (HL) center hosted by the Norwegian and Danish Meterologincal Institutes (met.no and DMI). This operational service has been running 24/7 since 2002. A major objective for the OSI SAF HL center is to provide global sea ice products derived from available operational satellites. These products are tailored for use in weather and ocean models, for environmental studies, ocean monitoring, etc... The OSI SAF provides a fully operational service with focus on high quality and routinely validated products, freely available for all users from `www.osi-saf.org`.

In this section, we shortly describe the specifications of the OSI SAF sea ice drift product and compare them to those of the ice drift products delivered by the French Institute for Marine Research, IFREMER (e.g. Ezraty et al. (2008)).

3.1. Satellite sensors

The OSI SAF low resolution sea ice drift products use SSM/I, AMSR-E and ASCAT[2]. Swaths recorded by these instruments are first averaged in a daily composite map, before ice motion vectors are computed from one image to another. The OSI SAF products are based on SSM/I 85 GHz brightness temperatures (T_B), ASCAT σ^0 and AMSR-E 37 GHz T_B. ASCAT σ^0 are corrected for view-angle variation. Those are the same sensors used at IFREMER, although Ezraty et al. (2007a) process ice motion vectors from the 89 GHz channels of AMSR-E, instead of the 37 GHz channels.

3.2. Temporal characteristics

Thanks to the CMCC (section 2), the OSI SAF products pertain of 2-day ice motion vectors. Specifically, each vector measures the Lagrangian net displacement from location ($\mathtt{lat}_0$,$\mathtt{lon}_0$) at time $\mathtt{t}_0$ to location ($\mathtt{lat}_1$,$\mathtt{lon}_1$) at time $\mathtt{t}_1 \approx \mathtt{t}_0$ + 48 h. The time lag of the motion vectors Δ_t is not exactly 48 hours and does vary from one sensor to the other and from place to place over the globe. The swath and scan patterns of the instrument determine the maps of $\mathtt{t}_0$, $\mathtt{t}_1$ and, thus, Δ_t. Gridded maps of $\mathtt{t}_0$ and $\mathtt{t}_1$ are distributed along with the OSI SAF ice drift product and correspond to an average observation time of ($\mathtt{lat}_0$,$\mathtt{lon}_0$) and ($\mathtt{lat}_1$,$\mathtt{lon}_1$) by the satellite sensor. The ice drift products from IFREMER are either 3- or 2-day data sets.

As discussed by Ezraty et al. (2007b), sea ice motion processing from those passive and active microwave sensors is challenged by increasing atmospheric perturbations (Cloud Liquid Water, CLW) and surface melting events (melt ponds) during Arctic summer. As for the IFREMER products, the OSI SAF sea ice drift products are not distributed from May to September. However, monthly validation statistics reported in Lavergne et al. (2010) concur with the findings of Kwok (2008) that the AMSR-E instrument might be used for shortening this period in the future.

3.3. Spatial characteristics

Similarly to the 3-day product from IFREMER, the OSI SAF ice drift vectors are distributed along a Polar Stereographic Earth mapping with 62.5 km grid spacing (Ezraty et al. 2007b). Furthermore, each motion vector corresponds to the area-average of motion of approximatively 140 km×140 km of ice surface around each grid location[3]. This area is similar to the one used for the 3-day product from IFREMER. Note that the 2-day product from IFREMER, being based on higher resolution AMSR-E 89 GHz images, achieves a smaller grid spacing between its motion vectors (32.5 km) and approximatively one fourth of the extent for the area averaging surface. The 89 GHz wavelength is, however, rather sensitive to atmospheric contamination and particularly to CLW content. For this reason, this data set seems to only reach its nominal quality, in terms of number of quality checked ice drift vectors in a daily grid, in the coldest months of Arctic winter (Ezraty et al. (2007a, Figure 8)). Another difference is in the spatial coverage. The IFREMER products cover the Arctic Ocean, while the OSI SAF grid covers the Northern Hemisphere, and thus also includes the Baffin and Hudson Bay as well as Bering and Okhotsk Sea.

3.4. Summary

Table 1 summarizes the characteristics of the OSI SAF and IFREMER sea ice drift products while figure 1 is an example OSI SAF multi-sensor (`OSI-407-MULTI`) sea

[2] A second OSI SAF sea ice drift product, labelled ”medium-resolution” is based on Metop AVHRR imagery.

[3] This area corresponds to extent of the tracking window (*aka* sub-image) of the cross-correlation algorithm

Table 1. Summary of main temporal and spatial characteristics of the OSI SAF and IFREMER sea ice drift products.

Identifier	Source	Duration [days]	Resolution [km]	Notes
`OSI-407-AMSR`	AMSR-E (37 GHz)	2	62.50	
`OSI-407-ASCAT`	ASCAT (σ^0)	2	62.50	
`OSI-407-SSMI`	SSM/I (85 GHz)	2	62.50	
`OSI-407-MULTI`	`OSI-407-*`	2	62.50	w&w/out gap-filling
`IFREMER-AMSR`	AMSR-E (89 GHz)	2	31.25	
`IFREMER-MRGD`	ASCAT and SSM/I	3	62.50	w&w/out gap-filling

ice drift product, using the CMCC and based on AMSR-E, SSM/I and ASCAT imagery.

4. VALIDATION IN THE ARCTIC

Validation of satellite-based sea ice drift products is traditionally conducted against trajectories of in situ platforms drifting with the ice pack. Two approaches are often reported upon. The Eulerian approach consists in validating daily maps of drift vectors against all corresponding in situ motion vectors, by accumulating the error statistics over a long enough period (months to years) to obtain robust statistics. The Lagrangian approach consists in following individual in situ drifters over extented periods (weeks to months) by concatenating the daily satellite ice drift vectors and thus in comparing two trajectories.

4.1. Validation: Eulerian approach

Eulerian-based validation results of the EUMETSAT OSI SAF ice drift products are reported at length by Lavergne et al. (2010). Both document practically unbiased and un-correlated 2D validation statistics against highly accurate GPS in situ trajectories in the Arctic. The standard deviation of the error statistics range from 2.5 to 4.5 km for both components of the drift vectors, depending on the sensor being processed and on the exact composition of the validation dataset. In any case, Lavergne et al. (2010) proove that those statistics are significantly better than those obtained from the very same satellite images, but using the MCC (see section 2), confirming the results one could visually assess from comparing figure 2 with 3. When using the CMCC, the sea ice motion information obtained from processing AMSR-E (37 GHz) imagery validates better against in situ measurements than those obtained from the SSM/I (85 GHz) or ASCAT (σ^0) imagery.

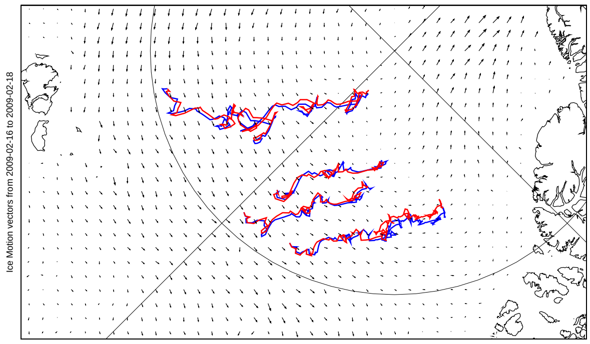

Figure 4. Lagrangian tracking of 6 ice-tethered drifters in the central Arctic over 6 months (from 1 October 2008 to 31 March 2009). The red trajectories pertain of position records of 6 ITPs, taken every two days at 1200 utc. The blue trajectories are obtained by concatenating the EUMETSAT OSI SAF 2-day multi-sensor *ice drift product. The trajectories follow the general pattern of the Trans-Polar drift (Fram Strait is towards the upper-right corner) but also exhibit some level of day-to-day variability, most probably imposed by variability in surface winds. The super-imposed ice motion vectors are from the 48-hour ice drift product from 16 to 18 February 2009.*

4.2. Validation: Lagrangian approach

The Lagrangian approach to validation gives further insight on the temporal consistency of the satellite product, as we track the position of an ice-tethered drifter by concatenating the satellite-based ice motion vectors over several months.

Figure 4 is an example 6-month Lagrangian tracking of 6 Ice Tethered Profilers (ITP) during winter 2008–2009 in the Arctic[4]. The close agreement between the in situ (red) and concatenated (blue) trajectories indicate that the accuracy of the OSI SAF product allow for tracking the parcels of the ice surface over extended period of time. The slowly growing distance between the red and blue curves is due to error accumulation, since the Lagrangian

[4]Four of the trajectories overlap in the direction of the Trans-Polar drift.

trajectory is first initialized at the same geographical position as the associated ITP but later drifts "freely", without further update on the location of the buoy.

It should be noted that the *multi-sensor* ice drift product was selected for this exercise (`OSI-407-MULTI` in table 1). The single-sensor products have good coverage as well, but might exhibit missing vectors that would halt the Lagrangian tracking. Graphs documenting the the density of valid vectors over the seasons can be found in Lavergne (2010, Chapter 5).

5. CONCLUSION

Thanks to their extended spatial coverage and high observation frequency, low resolution imaging sensors can still provide valuable information on sea ice motion for assimilation in coupled ocean and ice models. We briefly introduce the Continuous Maximum Cross-Correlation (CMCC) as a motion tracking methodology that takes advantage of a continuous formalism for removing the quantization noise. This quantization noise prevents the use of the well-known MCC method for computing Arctic ice motion vectors with short duration (3-day and less).

The CMCC was implemented in the operational processing chain of the EUMETSAT Ocean and Sea Ice Satellite Application Facility (OSI SAF, `www.osi-saf.org`). Since December 2009, daily sea ice drift products are available for the Northern Hemisphere, at a resolution of 62.5 km and with a time-span of 48 hours. At the time being, single-sensor ice drift products based on AMSR-E, SSM/I and ASCAT are processed and distributed, as well as a multi-sensor product that takes advantage of the 3 sensors mentionned above for minimizing the number of missing vectors in a daily grid.

Validation results are introduced that document the accuracy achieved by the OSI SAF products against in situ trajectories. Both Eulerian and Lagrangian approaches are reported upon.

Interested users can access the OSI SAF sea ice products and documentation from `http://osisaf.met.no` and read more details about the CMCC method and its validation results from Lavergne et al. (2010).

ACKNOWLEDGMENTS

This research work partly took place within the frame of the DAMOCLES project. The DAMOCLES project is financed by the European Union under the 6th Framework Programme for Research and Development. The research work also received support from the Norwegian Research Council through its International Polar Year programme and the project iAOOS Norway – Closing the Loop (grant number 176096/S30, `http://www.iaoos.no`). The European Commission also participated through the MERSEA Integrated Project, under the 6th Framework Program, Thematic Priority Space / GMES. Finally, the EUMETSAT Ocean and Sea Ice SAF (`http://www.osi-saf.org`) provided financial support during its Continuous Development and Operations Phase (CDOP).

The Ice-Tethered Profiler data were collected and made available by the Ice-Tethered Profiler Program based at the Woods Hole Oceanographic Institution `http://www.whoi.edu/itp`.

This work could not have been possible without the support of the Research and Development Division of the Norwegian Meteorological Institute.

REFERENCES

Bertino, L. & Lisæter, K. 2008, Mercator Ocean Quaterly Newsletter, 28, 41

Ezraty, R., Girard-Ardhuin, F., & Croizé-Fillon, D. 2007a, Sea ice drift in the central Arctic estimated using the 89 GHz brightness temperatures of the Advanced Microwave Scanning Radiometer – User's manual, v2.0, CERSAT, IFREMER, France

Ezraty, R., Girard-Ardhuin, F., & Piollé, J.-F. 2007b, Sea ice drift in the central Arctic estimated from Sea-Winds/QuikSCAT backscatter maps – User's manual, v2.2, CERSAT, IFREMER, France

Ezraty, R., Girard-Ardhuin, F., & Piollé, J.-F. 2008, Sea ice drift in the central Arctic combining QuikSCAT and SSM/I sea ice drift data – User's manual, v3.0, CERSAT, IFREMER, France

Kauker, F., Kaminski, T., Karcher, M., et al. 2009, Geophysical Research Letters, 36

Kwok, R. 2008, Geophysical Research Letters, 35

Lavergne, T. 2010, Validation and Monitoring of the OSI SAF Low Resolution Sea Ice Drift Product – v2, Tech. Rep. SAF/OSI/CDOP/met.no/T&V/RP/131, EUMETSAT OSI SAF – Ocean and Sea Ice Sattelite Application Facility

Lavergne, T., Eastwood, S., Teffah, Z., Schyberg, H., & Breivik, L.-A. 2010, Journal of Geophysical Research, xx, in press

Nelder, J. A. & Mead, R. 1968, Computational Journal, 7, 308

Notarstefano, G., Poulain, P.-M., & Mauri, E. 2007, Journal of Atmospheric and Oceanic Technology, 25, 271

Stark, J. D., Ridley, J., Martin, M., & Hines, A. 2008, Journal of Geophysical Research, 113